Optical-absorption spectra of the layered transition-metal thiophosphates MPS_3 (M = Mn, Fe, and Ni)

P. A. Joy and S. Vasudevan
Department of Inorganic and Physical Chemistry, Indian Institute of Science, Bangalore 560 012, India
(Received 17 December 1990; revised manuscript received 3 March 1992)

Optical-absorption spectra of single crystals of manganese, iron, and nickel thiophosphates have been recorded at 300 and 120 K. The spectral features have been assigned to transitions within the d-electron manifold of the corresponding metal ion in octahedral symmetry. The spectra have been analyzed with use of the weak-field coupling scheme of crystal-field theory and the transition energies have been calculated by diagonalization of the appropriate weak-field matrices. The crystal-field-splitting parameter Dq has been found to be similar in magnitude (~ 850 cm^{-1}) for all three compounds. The calculated values of the Racah interelectron repulsion parameter B for $MnPS_3$, $FePS_3$, and $NiPS_3$ are 560, 900, and 950 cm^{-1}, respectively, which are close to that of the corresponding free ion and that in other ionic compounds. The crystal-field parameters have thus been used to establish the covalency or ionicity of the M-S linkage in these compounds. All three compounds are ionic with the d states localized in character.

I. INTRODUCTION

Layered compounds have received considerable attention from the scientific community because of the wide range of chemical and physical properties that they exhibit. Among the various crystallographically layered compounds the transition-metal chalcogenophosphates,[1,2] MPX_3, where M is a first-row transition metal with an incomplete d shell (Mn, Fe, Ni, etc.) and X = S or Se, are perhaps unique since they are magnetic. The structure of the transition-metal thiophosphates, MPS_3, may be derived from that of the layered $CdCl_2$ structure[3] and is closely related to that of the transition-metal dichalcogenides. The structure consists of MPS_3 layers separated by a van der Waals gap. This allows the possibility of reversible and topotactic intercalation of various guest species between the layers.[1,4]

Although the MPS_3 compounds have been the subject of a number of spectroscopic studies—optical absorption,[5] reflection,[6] phosphorescence,[7] fluorescence,[8] x-ray photoelectron spectroscopy (XPS),[9] x-ray absorption spectroscopy (XAS),[10] ir, and Raman[11]—there are disagreements as to the degree of covalency or ionicity of the M-S linkages. Optical absorption, XPS, and x-ray absorption edge measurements have generally been interpreted assuming that the nature of interaction between metal and sulphur is ionic, the so-called weak interaction model. A study of the phosphorescence spectra[7] of $MnPS_3$, however, concluded that the material is fairly covalent. On the other hand, a more recent fluorescence spectroscopic study[8] of the same compound was found to be in agreement with the weakly interacting model. The question is whether to view the MPS_3 compounds as covalent solids like the transition-metal dichalcogenides or as ionic salts $[M_2^{2+}(P_2S_6)^{4-}]$ in which case the d electrons would be localized and atomic like.

In this paper we present a detailed study of the optical-absorption spectra (5000–50 000 cm^{-1}) of crystals of $MnPS_3$, $FePS_3$, and $NiPS_3$. The work was stimulated by the fact that a more quantitative understanding of the extent of covalency or ionicity of the M-S linkage is a prerequisite to an understanding of the intercalation in these compounds. In this spectral region the observed features correspond to transitions within the d-electron manifold of the corresponding transition-metal ion. We have calculated the various transition energies in the weak-field coupling scheme of crystal-field theory.[12] An *a priori* justification for adopting the weak-field coupling scheme comes from the magnetic data which showed that in $MnPS_3$, $FePS_3$, and $NiPS_3$ the transition-metal ions are in the divalent high spin state.[13] Agreement between the calculated and the observed spectral features was obtained for all three compounds, justifying the use of this coupling scheme. The Racah B and C interelectron repulsion parameters, as obtained from the calculation, showed that in all three compounds the transition-metal d states are localized and atomiclike.

II. EXPERIMENTAL

Single crystals of $MnPS_3$, $FePS_3$, and $NiPS_3$ were grown by the chemical vapor transport method.[14] Optical-absorption spectra of single crystals were recorded using a Hitachi U3400 recording spectrophotometer. Crystals of $MnPS_3$, $FePS_3$, and $NiPS_3$ were cleaved using adhesive tape to the required thickness and were fixed on an optically polished quartz disk using nujol and mounted inside a Specac P/N 21.000 variable temperature cell. The crystal ab plane was perpendicular to the incident beam ($\mathbf{E} \perp c$). Spectra were recorded at 300 and 120 K. A blank run was performed at these temperatures without the crystal, to correct for any background effect.

III. RESULTS

The optical-absorption spectra of $MnPS_3$ single crystal recorded at 300 and 120 K are shown in Fig. 1. A strik-

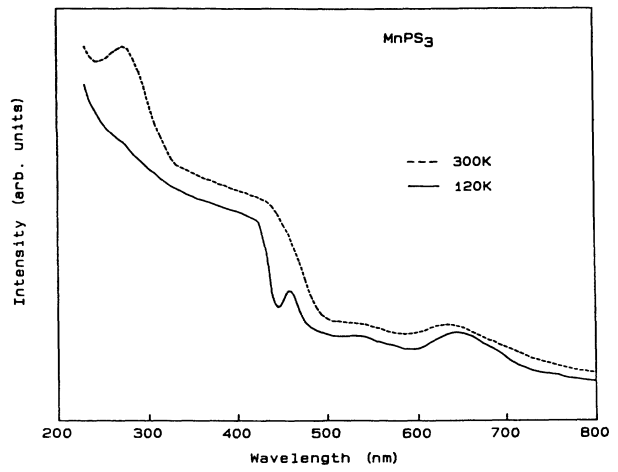

FIG. 1. Optical absorption spectra of single-crystal $MnPS_3$ at 120 and 300 K.

ing feature of the spectra is the much greater clarity at low temperature. In particular, there is a large blue shift and a sharpening in the onset of the intense absorption at about 440 nm (22 700 cm^{-1}). As a consequence, the absorption at 460 nm (21 835 cm^{-1}) is clearly resolved at low temperature. The weak absorption bands at 635 nm (15 748 cm^{-1}) and 515 nm (19 417 cm^{-1}) show no temperature dependence. The high-energy absorption at 268 nm (37 300 cm^{-1}) is seen only in the room-temperature spectrum. The overall temperature dependence shows a striking similarity to that of α-MnS,[15] even though the positions of the bands are different. The room-temperature optical spectra in the 12 500–25 000 cm^{-1} range have been previously reported by Grasso, Santangelo, and Piacentini.[5] The present spectra (10 000–40 000 cm^{-1}), however, are of much higher quality especially at low temperature.

The absorption spectrum of $FePS_3$ single crystal at 120 K in the near ir region is shown in Fig. 2(a). The spectrum is characterized by a broad intense transition at 1149 nm (8700 cm^{-1}). The optical-absorption spectrum in the visible and ultraviolet region recorded at 120 K is shown in Fig. 2(b). The spectrum of $FePS_3$ at 300 K showed only a few weak bands and has not been included in Figs. 2(a) and 2(b). Even at low temperature, the features are extremely weak and broad. Weak transitions are observed at 690 nm (14 490 cm^{-1}), 613 nm (16 300 cm^{-1}), 580 nm (17 241 cm^{-1}), 503 nm (19 880 cm^{-1}), 460 nm (21 739 cm^{-1}), 417 nm (23 981 cm^{-1}), and 376 nm (26 596 cm^{-1}) in the visible region and a number of weak bands in the ultraviolet region are also observed.

The electronic spectra of $NiPS_3$ at 300 and 120 K are shown in Fig. 3. It consists of a broad peak at 1123 nm (8900 cm^{-1}) and a steep absorption starting at 850 nm (11 765 cm^{-1}). Two other well-defined transitions occur at 382 nm (26 210 cm^{-1}) and 595 nm (16 800 cm^{-1}), respectively. At 120 K a very weak transition at 675 nm (14 765 cm^{-1}) is observed. There is a decrease in intensity of the absorption at 8900 cm^{-1} at low temperature. The high-energy absorption at 273 nm (36 650 cm^{-1}) also shows a strong temperature dependence, being most easily observed at 300 K.

IV. DISCUSSION

The spectra have been interpreted in terms of transitions within the d-electron manifold of the transition-metal ion in an octahedral field and have been analyzed in the weak-field limit of the crystal-field theory.[12] In this limit the electron-electron repulsion terms are considered to be much stronger than the crystal field. In the MPS_3 compounds the MS_6 polyhedra have a slight trigonal distortion[3] (the metal ion point group symmetry is lowered

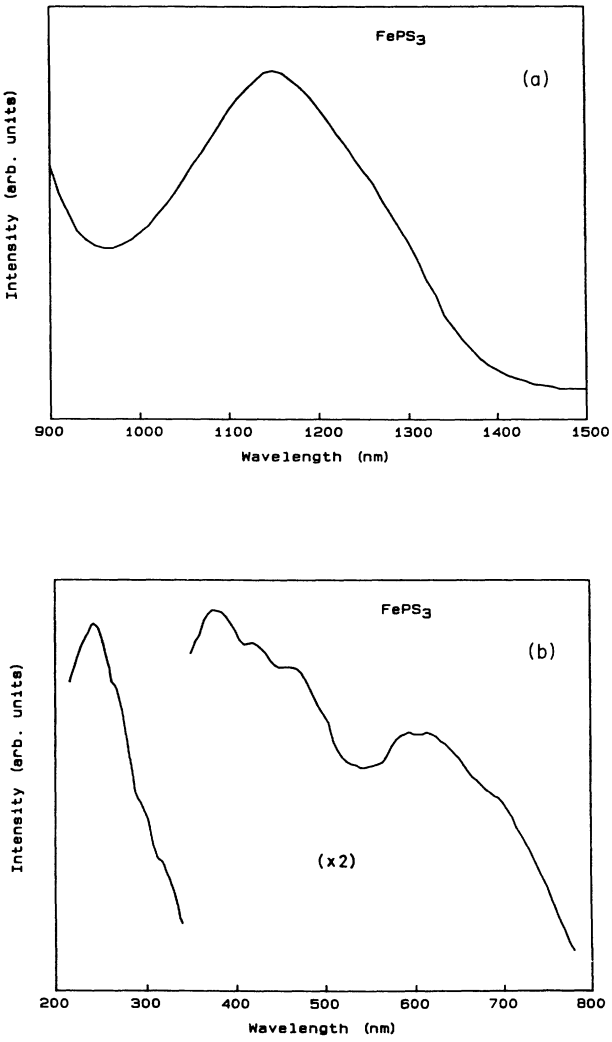

FIG. 2. (a) Optical-absorption spectra of $FePS_3$ crystal in the near infrared region at 120 K. (b) Optical-absorption spectra of $FePS_3$ crystal in the uv-visible region at 120 K.

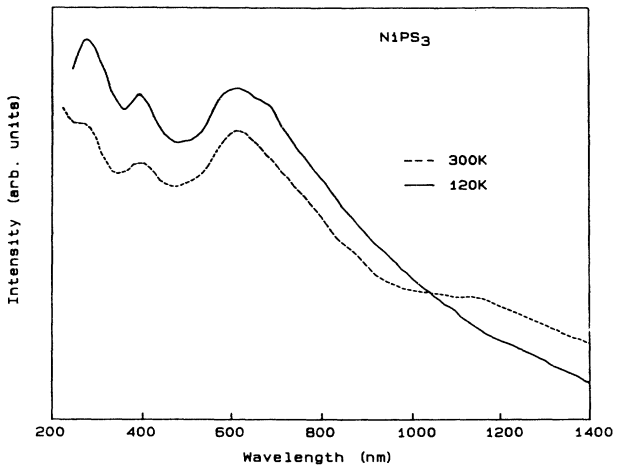

FIG. 3. Optical-absorption spectra of $NiPS_3$ single crystal at 120 and 300 K.

from O_h to D_{3d}). It is, however, extremely small and is likely to give rise to splittings of the order of 100 cm^{-1} or less and has consequently been neglected. Spin-orbit coupling, too, has not been included in the calculations except in the case of $NiPS_3$, where the effect is not negligible. The spin-orbit coupling constant for the free ions[12] Mn^{2+} and Fe^{2+} lies within 100 cm^{-1}, whereas for Ni^{2+} the value is about 300 cm^{-1}. The transition energies for the d^5, d^6, and d^8 ions were obtained by diagonalizing the appropriate weak-field matrices. The elements of the matrices are expressed as a function of Dq, the crystal-field-splitting parameter, and B and C, the Racah interelectron repulsion parameters.[16] For a $3d$ ion, B and C are related to the Slater-Condon parameters F_2 and F_4 by the linear relations[17] $C=35F_4$ and $B=F_2-5F_4$. These parameters were varied till agreement between the calculated and observed energies obtained. A comparison of the B and C values, so obtained, with that of the corresponding values for the free ion, and for the ions in similar compounds, can be used to establish the extent of covalency felt by the d electrons, since it is well known[18] that on compound formation the decrease in B from the free ion value is a measure of the covalency of the d electrons.

A. $MnPS_3$

For an Mn^{2+} ion (d^5 system), the ^6S free ion ground-state transforms as the $^6A_{1g}$ in an octahedral crystal field. The next higher free ion states, in the order of increasing energy, are the quartet states ^4G, ^4D, ^4P, and ^4F. In the presence of an octahedral crystal field, these states are split to various levels. The various bands in the absorption spectra may be considered to be due to electronic transitions from the $^6A_{1g}$ ground state to the higher-lying quartet states.

In interpreting the spectra, the main points to be noted are (i) The ^6S ground state is not split by the crystal field and consequently the absorptions are due to sextet-quartet transitions. Since these transitions are spin forbidden, the absorptions are expected to be very weak, and (ii) a large blue shift with decreasing temperature may be expected for transitions involving charge transfer between ligand and metal or vice versa, whereas the transitions involving only the Mn^{2+} states would show very little temperature dependence.[15]

The absence of temperature shifts for the first three bands at 635 nm (15 748 cm^{-1}), 515 nm (19 417 cm^{-1}), and 460 nm (21 835 cm^{-1}) is a strong evidence for them being internal crystal-field transitions in the Mn^{2+} ion. These bands are assigned as $^6A_{1g}\rightarrow{}^4T_{1g}$, $^6A_{1g}\rightarrow{}^4T_{2g}$, and $^6A_{1g}\rightarrow{}^4A_{1g}$ and ^4E_g transitions, respectively; these quartet states arising from the free ion ^4G term. The absorption edge at 440 nm (22 700 cm^{-1}) and the high-energy peak at 268 nm (37 300 cm^{-1}), both of which show a strong temperature dependence, are assigned to charge-transfer bands. Since they are not seen in the Mn^{2+} phosphorescence spectra,[7] they are probably ligand to metal in origin.

The crystal-field bands have been interpreted in the weak-field limit rather than the strong field. The main reasons for doing this are the following (i) The position of the $^6A_{1g}\rightarrow{}^4A_{1g}$ and ^4E_g band, which is sensitive to the ionicity of the compound, is comparable to that in the manganese halides[19] ($MnBr_2$ 435 nm, $MnPS_3$ 458 nm). For a free ion,[20] this occurs at 372 nm (26 850 cm^{-1}). (ii) It has been shown that in covalent manganese compounds[21] the e_g d electrons would engage in stronger covalent interactions than the t_{2g} d electrons. Consequently the Racah parameters for these electrons would be different, leading to a splitting of the initially degenerate $^4A_{1g}$ and ^4E_g levels. The observed peak at 460 nm (21 835 cm^{-1}), which is sufficiently sharp and well resolved, shows no such splitting. In the light of the above arguments it appears, then, that $MnPS_3$ is fairly ionic and the weak-field interpretation is more appropriate.

The weak-field energy matrices for a d^5 system[22] are diagonalized and the various transition energies obtained are compared with the experimental results. For $MnPS_3$, the values so obtained were $Dq=850$ cm^{-1}, $B=560$ cm^{-1}, and $C=3250$ cm^{-1}. The observed and calculated energies for the transitions are listed in Table I. The splittings of the various free ion terms of the Mn^{2+} ion in a weak field of octahedral symmetry are calculated as a function of Dq for the above B and C values and are shown in Fig. 4. From a comparison of the B values (Table II), it may be seen that $MnPS_3$ is comparable in ionicity to α-MnS.

An earlier strong-field calculation,[7] based on the phosphorescence spectra, gave an exceptionally small value of B (494 cm^{-1}), well below that of other divalent manganese compounds, suggesting a high degree of covalency. The absorption spectra, however, show none of the features expected for highly covalent manganese compounds. Recently Grasso *et al.*[8] reported the fluores-

TABLE I. Calculated and observed transition energies for $MnPS_3$. $B = 560\ cm^{-1}$, $C = 3250\ cm^{-1}$, and $Dq = 850\ cm^{-1}$.

Calculated transition energy (cm^{-1})	Observed transition energy (cm^{-1})	Assignments
15 780	15 748	$^6A_{1g} \rightarrow {}^4T_{1g}(G)$
18 830	19 417	$^6A_{1g} \rightarrow {}^4T_{2g}(G)$
21 850	21 834	$^6A_{1g} \rightarrow {}^4A_{1g}$ and $^4E_g(G)$
	22 700	Charge transfer
24 100		$^6A_{1g} \rightarrow {}^4T_{2g}(D)$
25 770		$^6A_{1g} \rightarrow {}^4E_g(D)$
31 337		$^6A_{1g} \rightarrow {}^4T_{1g}(P)$
35 070		$^6A_{1g} \rightarrow {}^4A_{2g}(F)$
36 674		$^6A_{1g} \rightarrow {}^4T_{1g}(F)$
	37 300	Charge transfer
39 761		$^6A_{1g} \rightarrow {}^4T_{2g}(F)$

cence spectra of $MnPS_3$ crystal and calculated the B value as 600 cm^{-1}. Their calculations were, however, based on only the Dq independent transitions,[17]

$$^6A_{1g} \rightarrow {}^4A_{1g}, \quad \Delta E = 10B + 5C ,$$

$$^6A_{1g} \rightarrow {}^4E_g, \quad \Delta E = 17B + 5C .$$

The position of the first transition was obtained by the deconvolution of a single broad excitation spectra into four Gaussian components, whereas the latter is seen as an extremely broad peak at the limit of the excitation spectra. Since the B value depends mainly on the energy of these transitions, their results are likely to be less reliable than the present fitting procedure, where all observed transitions were considered.

TABLE II. The Racah interelectron repulsion parameter B for ionic Mn^{2+} compounds.

Compound	B (cm^{-1})	Reference
Mn^{2+} (free ion)	786	23
MnO	750	24
$(Mn(H_2O)_6)^{2+}$	671	23
$MnCl_2$	630	25
$MnBr_2$	536	26
MnS	583	15
$MnPS_3$	560	This work
	494	7
	600	8

B. $FePS_3$

The ground state of Fe^{2+} (d^6 system) free ions is ^5D. In an octahedral crystal field the ^5D ground state splits into $^5T_{2g}$ and ^5E_g, with the $^5T_{2g}$ being lower in energy. Electronic transitions from $^5T_{2g}$ to ^5E_g are spin allowed. The next higher-lying states of the free ion are the triplets; ^3H, ^3F, ^3P, ^3G, and ^3D. In a crystal field of octahedral symmetry, these states transform as the $^3T_{1g}$, $^3T_{2g}$, ^3E_g, $^3A_{2g}$,

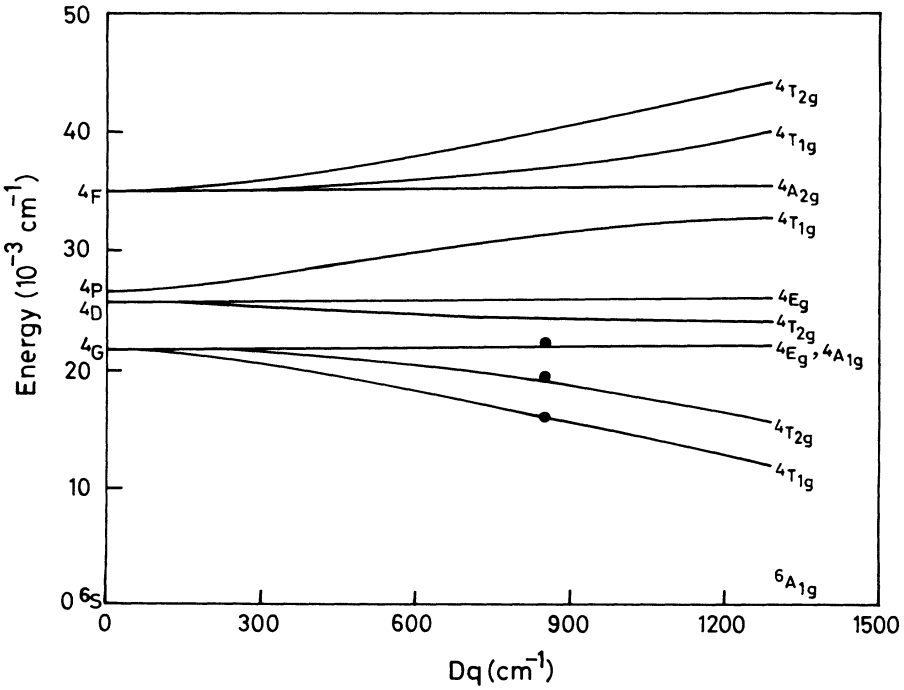

FIG. 4. Splitting of Mn^{2+} free ion terms by an octahedral crystal field. The curves were computed for $B = 560\ cm^{-1}$ and $C = 3250\ cm^{-1}$ by diagonalizing the weak-field matrices for a d^5 ion. The circles indicate the positions of the experimentally determined energy levels.

and $^3A_{1g}$ representations.

For Fe^{2+} ions in an octahedral symmetry, the only spin allowed transition is the $^5T_{2g} \rightarrow {}^5E_g$ transition. The other possible transitions are from the $^5T_{2g}$ level to the triplet levels. These are spin-forbidden transitions and are therefore expected to be very weak, but exchange interactions may cause an increase in intensity. For example, in the linear chain $M\mathrm{Fe}X_3$ compounds,[27] the intensity of the spin-allowed and spin-forbidden transitions are comparable and have been explained in terms of a cooperative exchange mechanism involving adjacent transition-metal ions. In $FePS_3$, however, no exchange enhancement of the intensity of spin-forbidden transitions was observed. It may be seen from Fig. 2(b) that all transitions in the visible and ultraviolet region are weak and very broad. These transitions correspond to transitions from the ground state ($^5T_{2g}$) to the triplet manifold arising from the free ion ^3H, ^3P, ^3F, ^3G, and ^3D terms.

The intense peak in the $FePS_3$ spectrum at 1149 nm (8700 cm^{-1}) is assigned to the spin-allowed $^5T_{2g} \rightarrow {}^5E_g$ transition. Since the energy separation between the $^5T_{2g}$ and ^5E_g is $10Dq$, the crystal-field-splitting parameter, Dq, is obtained as 870 cm^{-1}. This agrees with the previous results of Banda[28] and Grasso, Santangelo, and Piacentini.[5] The $FePS_3$ spectra were interpreted in the weak-field limit of the crystal-field theory. The justification for this is as follows. Assuming that the strong field is applicable, the transitions at 690 nm (14 490 cm^{-1}) and 580 nm (17 241 cm^{-1}) may be assigned, following Banda,[28] to $^5T_{2g} \rightarrow {}^3T_{1g}$ and $^5T_{2g} \rightarrow {}^3T_{2g}$. In the strong-field limit the energies of these transitions are given by[17]

$$-10Dq + 5B + 5C - 70B^2/10Dq = 14\,490\ ,$$

$$-10Dq + 13B + 5C - 106B^2/10Dq = 17\,241\ .$$

Solving the above equations, one obtains B as 900 cm^{-1}. This value of B is quite large for the strong-field limit with $Dq/B \sim 1$. An examination of the Tanabe-Sugano diagram[29] for a d^6 ion in an octahedral field shows that when $Dq/B < 2$, the weak-field limit is more appropriate. Thus the spectral transitions in $FePS_3$ are assigned using the weak-field method.

The weak-field energy matrices of Ferguson *et al.*[31] for the triplet states are diagonalized and best-fit values were obtained for $Dq = 870$ cm^{-1}, $B = 900$ cm^{-1}, and $C = 4200$ cm^{-1}. Using the values of B and C, the Fe^{2+} energy levels of the triplet states are calculated as a function of Dq. This is shown in Fig. 5. The observed transitions in the visible and ultraviolet regions are assigned in the order $^3T_{1g}(H)$, $^3T_{2g}(H)$, $^3T_{1g}(H)$, $^3T_{2g}(F)$, $^3T_{1g}(P)$, $^3E_g(H)$, $^3T_{2g}(G)$, etc. The observed and calculated transition energies are given in Table III along with their assignments. The best agreement with experiment was obtained for a Dq value of 870 cm^{-1}. This is identical to the value of Dq obtained independently from the $^5T_{2g} \rightarrow {}^5E_g$ transition, whose energy is independent of the Racah parameters. Spin-forbidden transitions of high-spin Fe^{2+} (d^6) have rarely been studied, probably because of the weak nature of the spin-forbidden quintet-triplet transitions.[17] Pollini, Spinolo, and Benedek[30] have studied the vibronic structure of iron dihalides at liquid-helium temperature. They have observed sufficiently

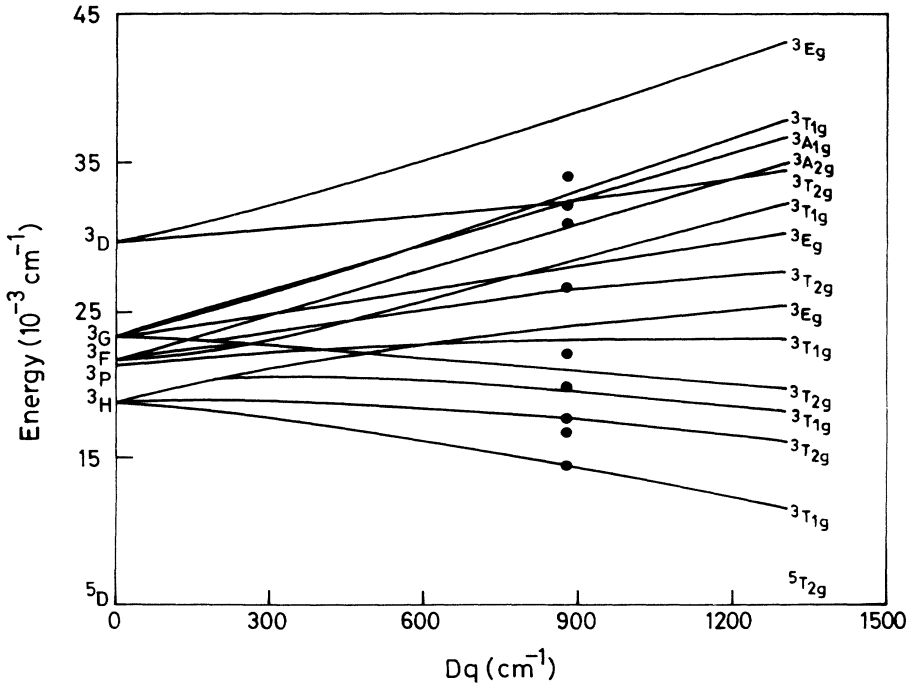

FIG. 5. Triplet manifold of a Fe^{2+} free ion split by an octahedral crystal field. The curves were computed for $B = 900$ cm^{-1} and $C = 4200$ cm^{-1} by diagonalizing the weak-field matrices for a d^6 ion. The circles indicate the positions of the experimentally determined energy levels.

TABLE III. Calculated and observed transition energies for $FePS_3$. $B = 900\ cm^{-1}$, $C = 4200\ cm^{-1}$, and $Dq = 870\ cm^{-1}$.

Calculated transition energy (cm^{-1})	Observed transition energy (cm^{-1})	Assignments
8 700	8 700	$^5T_{2g} \rightarrow {}^5E_g(D)$
14 353	14 490	$^5T_{2g} \rightarrow {}^3T_{1g}(H)$
	16 300	
17 534	17 241	$^5T_{2g} \rightarrow {}^3T_{2g}(H)$
19 369	19 880	$^5T_{2g} \rightarrow {}^3T_{1g}(H)$
20 837	21 739	$^5T_{2g} \rightarrow {}^3T_{2g}(F)$
22 888		$^5T_{2g} \rightarrow {}^3T_{1g}(P)$
23 711	23 981	$^5T_{2g} \rightarrow {}^3E_g(H)$
26 105	26 596	$^5T_{2g} \rightarrow {}^3T_{2g}(G)$
27 690		$^5T_{2g} \rightarrow {}^3E_g(G)$
28 034		$^5T_{2g} \rightarrow {}^3T_{1g}(F)$
30 328	30 395	$^5T_{2g} \rightarrow {}^3A_{2g}(F)$
	31 546	
32 010		$^5T_{2g} \rightarrow {}^3A_{1g}(G)$
32 081		$^5T_{2g} \rightarrow {}^3T_{2g}(D)$
32 503		$^5T_{2g} \rightarrow {}^3T_{1g}(G)$
	34 246	
	36 500	Charge transfer

TABLE IV. Calculated and observed transition energies for $NiPS_3$. $B = 950\ cm^{-1}$, $C = 4900\ cm^{-1}$, and $Dq = 890\ cm^{-1}$.

Calculated transition energy (cm^{-1})	Observed transition energy (cm^{-1})	Assignments
8 900	8 900	$^3A_{2g}(F) \rightarrow {}^3T_{2g}(F)$
14 896	14 765	$^3A_{2g}(F) \rightarrow {}^3T_{1g}(F)$
16 803	16 800	$^3A_{2g}(F) \rightarrow {}^1E_g(D)$
25 362		$^3A_{2g}(F) \rightarrow {}^1T_{2g}(D)$
26 234	26 210	$^3A_{2g}(F) \rightarrow {}^3T_{1g}(P)$
30 138		$^3A_{2g}(F) \rightarrow {}^1T_{1g}(G)$
	36 650	Charge transfer
36 825		$^3A_{2g}(F) \rightarrow {}^1E_g(G)$
37 256		$^3A_{2g}(F) \rightarrow {}^1T_{2g}(G)$

sharp transitions to the triplet states. The B value obtained for $FePS_3$ is close to that of the well-studied ionic $MFeX_3$ linear chain systems[27,31] ($RbFeF_3$ 945 cm^{-1}, $CsFeCl_3$ 875 cm^{-1}, $RbFeBr_3$ 900 cm^{-1}).

C. $NiPS_3$

The free ion ground term of Ni^{2+} (d^8 system) is the triplet ^3F state. In an octahedral crystal field, this level splits into $^3A_{2g}$, $^3T_{2g}$, and $^3T_{1g}$, of which $^3A_{2g}$ is the ground state. The next higher-energy states ^1E_g and $^1T_{2g}$, in octahedral symmetry, arise from the singlet ^1D free ion term while the $^3T_{1g}$ arising from the free ion ^3P state lies still higher in energy. Three spin-allowed transitions are possible for Ni^{2+}. These are the transitions from the ground state $^3A_{2g}$ to the levels $^3T_{2g}(F)$, $^3T_{1g}(F)$, and $^3T_{1g}(P)$. Usually for Ni^{2+} systems in octahedral symmetry, two spin-forbidden bands are also observed

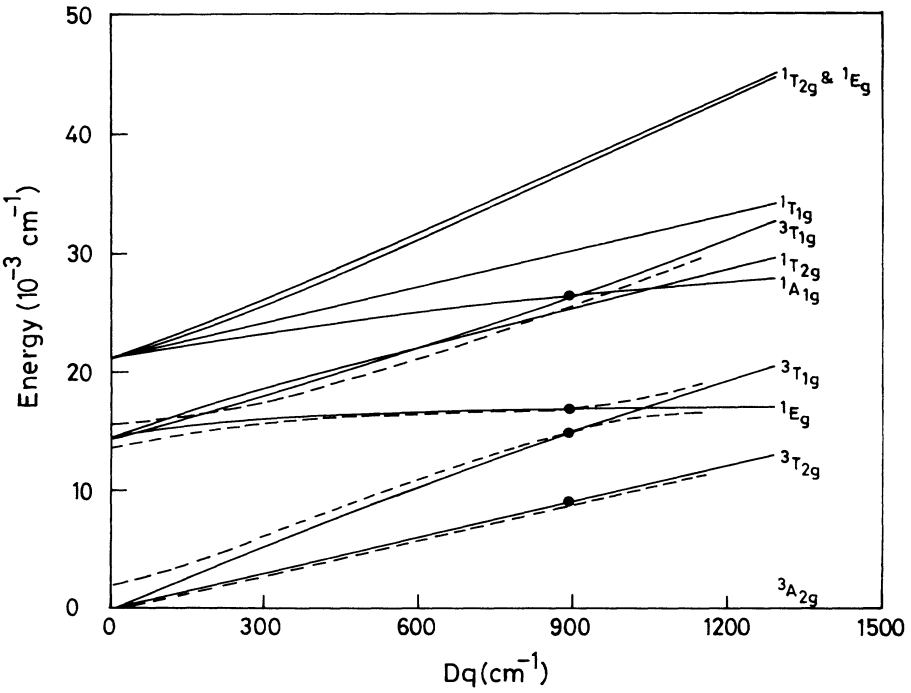

FIG. 6. Splitting of Ni^{2+} free ion terms by an octahedral crystal field. The solid curves were computed in the absence of spin-orbit coupling with $B = 950\ cm^{-1}$ and $C = 4900\ cm^{-1}$ by diagonalizing the weak-field matrices for a d^8 ion. The dashed lines are with spin-orbit coupling included for the same B and C values, and $\lambda = -280\ cm^{-1}$ (see text for details). Circles indicate the positions of the experimentally determined energy levels.

TABLE V. Calculated and observed transition energies for $NiPS_3$, with spin-orbit coupling included (Γ_3 and Γ_5 only). $Dq=890$ cm^{-1}, $F_2=1650$ cm^{-1}, $F_4=140$ cm^{-1}, $\lambda=-280$ cm^{-1}, $B=F_2-5F_4=950$ cm^{-1}, and $C=35F_4=4900$ cm^{-1}.

Calculated transition energy (cm^{-1})	Observed transition energy (cm^{-1})	Assignments
8 667	8 900	$\Gamma_5\rightarrow\Gamma_3$
9 121		$\Gamma_5\rightarrow\Gamma_5$
14 878	14 765	$\Gamma_5\rightarrow\Gamma_3$
15 131		$\Gamma_5\rightarrow\Gamma_5$
16 903	16 800	$\Gamma_5\rightarrow\Gamma_3$

from $^3A_{2g}$ to the states $^1E_g(D)$ and $^1T_{2g}(D)$. For a d^8 system, both weak- and strong-field methods give identical results. Since $MnPS_3$ and $FePS_3$ were analyzed in the weak-field limit, the same method is followed for $NiPS_3$.

All the transitions in the $NiPS_3$ absorption spectrum are very weak. The band at 1123 nm (8900 cm^{-1}) is assigned to the $^3A_{2g}\rightarrow{}^3T_{2g}$ transition and is a direct measure of the crystal-field-splitting parameter $10Dq$. The other bands at 660 nm (14 765 cm^{-1}), 595 nm (16 800 cm^{-1}), and 382 nm (26 210 cm^{-1}) are assigned as $^3A_{2g}\rightarrow{}^3T_{1g}(F)$, $^3A_{2g}\rightarrow{}^1E_g(D)$, and $^3A_{2g}\rightarrow{}^3T_{1g}(P)$ transitions, respectively. The feature at 273 nm (36 650 cm^{-1}), which shows a strong temperature dependence, is probably a charge-transfer band involving ligand states. It is interesting to note that this band appears at the same energy ($\sim$36 000 cm^{-1}) for all three compounds.

A weak-field analysis was performed using the matrices of Orgel[22] for a d^8 ion. Reasonable agreement with the experiment was obtained for $Dq=890$ cm^{-1} and the Racah parameters $B=950$ cm^{-1} and $C=4900$ cm^{-1}. The calculated and observed transition energies along with their assignments are given in Table IV. The weak-field splitting of the Ni^{2+} states, calculated as a function of Dq is shown in Fig. 6. It may be seen from the figure that the energies correspond to a Dq value of 890 cm^{-1}, which is identical to that obtained independently from the $^3A_{2g}\rightarrow{}^3T_{2g}$ transition.

In the preceding analysis the band at 595 nm (16 800 cm^{-1}), which appears with considerable intensity, had been assigned to the spin-forbidden $^3A_{2g}\rightarrow{}^1E_g(D)$ transition. Such spin-forbidden transitions have been observed in a number of other Ni^{2+} compounds[17] and are supposed to arise from spin-orbit coupling, which mixes the $^1E_g(D)$ and $^3T_{2g}(F)$ states. If may be seen from Fig. 6 that when Dq/B is close to unity ($Dq/B=0.94$ for $NiPS_3$) these levels are very close and extensive mixing may take place because of spin-orbit coupling. It is then strictly no longer correct to assign the bands as transitions to the states, ^1E_g and $^3T_{2g}$, because spin-orbit coupling mixes the two states.

By using the matrices of Liehr and Ballhausen[32] and the experimentally determined positions of the spin-orbit mixed "^1E" and "$^3T_2$" states, it has been possible to determine the spin-orbit coupling constant, λ, as well as an additional set of Racah parameters. In solving for these matrices, the value of Dq was taken as 890 cm^{-1}. Matrix diagonalization was carried out for various values of B, C, and λ. The best agreement with experiment was obtained for $B=950$ cm^{-1}, $C=4900$ cm^{-1}, and $\lambda=-280$ cm^{-1}. The calculated values for the transitions are given in Table V. The energies corresponding to the spin-orbit mixed states are shown as dashed lines in Fig. 6.

Both B and λ values for $NiPS_3$ show a similar trend, being fairly close to the free ion values. The Racah parameter B for $NiPS_3$ is comparable to those reported for other Ni^{2+} ionic salts ($[Ni(H_2O)_6]^{2+}$ 930 cm^{-1} (Ref. 33), $KNiF_3$ 990 cm^{-1} (Ref. 34), NiF_2 970 cm^{-1} (Ref. 35)). λ is very close to that of the free ion,[12] λ_0, -315 cm^{-1}. Thus both B and λ values suggest that in $NiPS_3$, the interaction between the Ni atoms and the ligands are ionic.

The results of the weak-field analysis of the optical spectra of the transition-metal thiophosphates $MnPS_3$, $FePS_3$, and $NiPS_3$ are summarized in Table VI. It may be seen that the B parameters for these compounds are close to the corresponding free ion values and so too are λ and λ_0. Thus in all three compounds the metal ions are in an ionic environment.

That the nature of M-S interactions in all three compounds are similar is also reflected in the calculated values of the crystal-field-splitting parameter, Dq (Table VI), which are similar in magnitude. All other factors being the same, the crystal-field splitting, Dq, should be proportional to the inverse of the M-S bond length. This is indeed found to be the case. $NiPS_3$, which has the shortest M-S bond length (2.463 Å), has the largest

TABLE VI. Calculated crystal-field parameters of transition-metal thiophosphates.

Compound	Dq (cm^{-1})	B (cm^{-1})	C (cm^{-1})	B_0 (cm^{-1})
$MnPS_3$	850	560	3250	786[a]
$FePS_3$	870	900	4200	1058[b]
$NiPS_3$	890	950 ($\lambda=-280$ cm^{-1})	4900	1084[b] ($\lambda_0=-315$ cm^{-1})[c]

[a]Reference 23.
[b]Reference 36.
[c]Reference 12.

crystal-field splitting (890 cm^{-1}), while $MnPS_3$, with the largest bond length (2.625 Å), of the three compounds, has the smallest crystal-field splitting (850 cm^{-1}). Thus optical-absorption spectra show that the MPS_3 compounds are ionic and the transition-metal d electrons are localized and atomiclike.

ACKNOWLEDGMENTS

The authors thank the Department of Science and Technology, Government of India, for financial assistance. One of us (P.A.J.) is grateful to CSIR, India, for partial support.

[1]J. W. Johnson, in *Intercalation Chemistry,* edited by M. S. Whittingham and A. J. Jacobson (Academic, New York, 1982), pp. 267-283.

[2]W. Klingen, R. Ott, and H. Hahn, Z. Anorg. Allg. Chem. **396**, 271 (1973).

[3]W. Klingen, G. Eulenberger, and H. Hahn, Z. Anorg. Allg. Chem. **401**, 97 (1973).

[4]R. Brec, Solid State Ionics **22**, 3 (1986).

[5]V. Grasso, S. Santangelo, and M. Piacentini, Solid State Ionics **20**, 9 (1986).

[6]F. S. Khumalo and H. P. Hughes, Phys. Rev. B **23**, 5375 (1981).

[7]J. B. Goates, E. Lifshitz, and A. H. Francis, Inorg. Chem. **20**, 3019 (1981).

[8]V. Grasso, F. Neri, L. Silipigni, and M. Piacentini, Phys. Rev. B **40**, 5529 (1989).

[9]M. Piacentini, F. S. Khumalo, G. Leveque, C. G. Olson, and D. W. Lynch, Chem. Phys. **72**, 61 (1982).

[10]Y. Ohno and S. Nakai, J. Phys. Soc. Jpn. **54**, 3591 (1985); Y. Ohno and K. Hirama, J. Solid State Chem. **63**, 258 (1986).

[11]G. K Kliche, J. Solid State Chem. **51**, 118 (1976); M. Jouanne and C. Julien, J. Appl. Phys. **64**, 3637 (1988); M. Scagliotti, M. Jouanne, M. Balkanski, G. Ouvrard, and G. Benedek, Phys. Rev. B **35**, 7097 (1987); C. Sourisseau, J. P. Forgerit, and Y. Mathey, J. Solid State Chem. **49**, 134 (1983); M. Bernasconi, G. L. Marra, G. Benedek, L. Miglio, M. Jouanne, C. Julien, M. S. Scagliotti, and M. Balkanski, Phys. Rev. B **38**, 12 089 (1988).

[12]J. S. Griffith, *The Theory of Transition Metal Ions* (Cambridge University Press, Cambridge, 1961).

[13]G. Le Flem, R. Brec, G. Ouvrard, A. Louisy, and P. Segransen, J. Phys. Chem. Solids **43**, 455 (1982).

[14]B. E. Taylor, J. Steger, and A. Wold, J. Solid State Chem. **7**, 461 (1973); R. Nitsche and P. Wild, Mat. Res. Bull. **5**, 419 (1970).

[15]R. A. Ford, E. Kauer, A. Rabenau, and D. A. Brown, Ber. Bunseng. Phys. Chem. **67**, 460 (1963).

[16]G. Racah, Phys. Rev. **62**, 438 (1942).

[17]A. B. P. Lever, *Inorganic Electronic Spectroscopy* (Elsevier, Amsterdam, 1984), p. 507.

[18]C. K. Jorgenson, *Modern Aspects of Ligand Field Theory* (North-Holland, Amsterdam, 1971).

[19]R. Pappalardo, J. Chem. Phys. **31**, 1050 (1959).

[20]C. E. Moore, *Atomic Energy Levels,* Natl. Bur. Stand. (U.S.) Circ. No. 467 (U.S. GPO, Washington, DC, 1971), p. 37.

[21]S. Koide and M. K. L. Pryce, Philos. Mag. **3**, 607 (1958).

[22]L. E. Orgel, J. Chem. Phys. **23**, 1004 (1955).

[23]L. J. Heidt, G. F. Koster, and A. M. Johnson, J. Am. Chem. Soc. **80**, 6471 (1958).

[24]G. W. Pratt and R. Coelho, Phys. Rev. **116**, 281 (1959).

[25]K. E. Lawson, J. Chem. Phys. **44**, 4159 (1966).

[26]F. A. Cotton, D. M. L. Goodgame, and M. Goodgame, J. Am. Chem. Soc. **84**, 167 (1962).

[27]C. F. Putnik, G. M. Cole, B. B. Garret, and S. L. Holt, Inorg. Chem. **15**, 826 (1976).

[28]E. J. K. B. Banda, Phys. Status Solidi B **138**, K125 (1986).

[29]Y. Tanabe and S. Sugano, J. Phys. Soc. Jpn. **9**, 753 (1954).

[30]I. Pollini, G. Spinolo, and G. Benedek, Phys. Rev. B **22**, 6369 (1980).

[31]J. Ferguson, H. J. Guggenheim, and E. R. Krausz, Aust. J. Chem. **22**, 1809 (1969).

[32]A. D. Liehr and C. J. Ballhausen, Ann. Phys. (N.Y.) **6**, 134 (1959).

[33]A. Bose and R. Chatterjee, Proc. Phys. Soc. **83**, 23 (1963).

[34]J. Ferguson and H. J. Guggenheim, J. Chem. Phys. **44**, 1095 (1966).

[35]J. Ferguson, H. J. Guggenheim, H. Kamimura, and Y. Tanabe, J. Chem. Phys. **42**, 775 (1965).

[36]A. Abragam and B. Bleaney, *EPR of Transition Ions* (Clarendon, Oxford, 1970).